PHYSICAL REVIEW
LETTERS

VOLUME 74 13 FEBRUARY 1995 NUMBER 7

Index of Refraction of Various Gases for Sodium Matter Waves

Jörg Schmiedmayer,[1,2] Michael S. Chapman,[1] Christopher R. Ekstrom,[1] Troy D. Hammond,[1] Stefan Wehinger,[1,2] and David E. Pritchard[1]

[1]*Department of Physics and Research Laboratory of Electronics, Massachusetts Institute of Technology, Cambridge, Massachusetts 02139*

[2]*Institut für Experimentalphysik, Universität Innsbruck, A-6020 Innsbruck, Austria*

(Received 29 June 1994)

By inserting a gas cell in one arm of an atom interferometer, we have measured both the attenuation and the phase shift of a sodium matter wave that passes through monatomic (He, Ne, Ar, Kr, and Xe) or molecular gases (N_2, CO_2, NH_3, and H_2O). This determines the complex index of refraction for Na matter waves and, more accurately, the ratio of the real to the imaginary part of the forward scattering amplitude. These measurements are compared with several semiclassical scattering models.

PACS numbers: 03.75.Dg, 07.60.Ly, 34.20.Cf

Atom interferometers are becoming a powerful tool in the field of atomic physics [1]. Their applicability in this field is significantly increased if the two interfering components of the atom wave are physically separated by a physical barrier [2] allowing different interactions to be applied to each of the two components with a resulting shift of the interference pattern. This enables us to study interactions that shift the energy or phase for a *single* state of an atom with spectroscopic precision.

We have used this new capability to measure the index of refraction seen by sodium matter waves traveling through a gas sample, thus solving an old problem in atomic physics: determination of the collision-induced phase shift for ground state atoms. We find that the collision-induced phase shift for sodium atom waves passing through a variety of target gases is much more strongly dependent on the collision partner than the previously measured cross sections [3]. We present novel semiclassical calculations of this phase shift that show it to be very sensitive to the *shape* of the long range interatomic potential. Thus information from phase shift experiments may add significant information to long standing problems like solving ambiguities in the inversion of the scattering problem [4], attempts to interpret other data sensitive to the long range interatomic potential [5], and to collective effects in a weak interacting gas [6].

From the perspective of wave optics the evolution of the wave function Ψ while propagating through a medium is given by

$$\Psi(x) = \Psi(0) e^{ik_{\mathrm{lab}}x} e^{i(2\pi/k_c)Nx\,\mathrm{Re}[f(k_c,0)]} e^{-(2\pi/k_c)Nx\,\mathrm{Im}[f(k_c,0)]}. \quad (1)$$

Here k_{lab} is the wave vector in the laboratory frame, k_c is the wave vector in the center of mass frame of the collision, N is the density of the medium, and $f(k_c,0)$ is the forward scattering amplitude. The amplitude of Ψ is attenuated in proportion to the *imaginary* part of the forward scattering amplitude, which is related to the total scattering cross section, $\sigma_{\mathrm{tot}} = (4\pi/k_c)\,\mathrm{Im}[f(k_c,0)]$, by the optical theorem. In addition, there is a phase shift, $\Delta\varphi(x) = (2\pi/k_c)Nx\,\mathrm{Re}[f(k_c,0)]$, proportional to the *real* part of the forward scattering amplitude. In analogy to light optics one finds the complex index of refraction, $n = 1 + (2\pi/k_{\mathrm{lab}}k_c)Nf(k_c,0)$. The refractive index of matter for de Broglie waves has been demonstrated in electron holography [7] and extensively studied in neutron optics [8], especially using neutron interferometers [9]. In neutron optics, scattering is dominantly s wave and measuring the refractive index gives information about the scattering length.

In atom-atom scattering at thermal energies several hundred partial waves contribute. The real and imaginary parts of the scattering amplitude in the forward direction

are

$$\mathrm{Re}[f(k,0)] = \frac{1}{2k}\sum_{l=0}^{\infty}(2l+1)\sin 2\delta_l\,, \tag{2a}$$

$$\mathrm{Im}[f(k,0)] = \frac{1}{2k}\sum_{l=0}^{\infty}(2l+1)2\sin^2\delta_l\,, \tag{2b}$$

where δ_l is the phase shift of the partial wave with angular momentum l. Because the rapidly oscillating $\sin 2\delta_l$ term in Eq. (2a) averages to zero at smaller impact parameters, the main contribution to $\mathrm{Re}[f(k,0)]$ comes from *large* impact parameters, where the phase shift is less than π. In contrast, the $\sin^2\delta_l$ term in Eq. (2b) averages to $\frac{1}{2}$ for impact parameters inside the point at which $\delta_l = \pi$. $\mathrm{Im}[f(k,0)]$ and therefore the total cross section is basically determined by the location of this point. Our measurements show that $\mathrm{Re}[f(k,0)]$ varies substantially more than $\mathrm{Im}[f(k,0)]$ with the collision system and the theoretical models discussed in this Letter show that it gives new information about the *shape* of the long range potential.

We have measured $f(k,0)$ directly using our interferometer [10], built from three nanofabricated 200 nm period transmission gratings [11]. For this experiment we installed a new 10 cm long interaction region which consists of a 10 μm thick aluminized mylar foil stretched symmetrically between two side plates and positioned between the separated atom wave components downstream of the second grating. One side plate has an inlet in the center for the introduction of gas as well as end tabs that restrict the openings at the entrance and exit to only 200 μm (Fig. 1). This allows us to send one portion of the atom wave through a gas target of up to $\sim 10^{-3}$ torr without noticeably disturbing the other portion. With the interaction region in place, we have observed fringes with 30% contrast and an interference amplitude of more than 3500 counts/s. We can determine the phase of the interference pattern with a precision of 5 mrad in one min. In spite of the many partial waves (typical $l_{\max}$ is a few hundred) involved, we are justified in considering only forward scattering in this experiment because the smallest features in the differential scattering amplitude are in the order of $1/l_{\max} > 1$ mrad, which is much larger than the angular acceptance of our interferometer (30 μrad). Therefore we are exclusively sensitive to $f(k,0)$.

We performed two separate measurements. One determined the attenuation of the beam intensity (proportional to σ_{tot}) which together with the cross sections from Ref. [12] allows us to estimate the gas density. The other measured the phase shift $\Delta\phi$ and the attenuation of the amplitude of the wave function that passed through the gas.

For the first experiment the transmission of the beam through the gas cell was measured as a function of gas pressure. The mylar foil of the interaction region was positioned in the diffraction pattern formed by the first

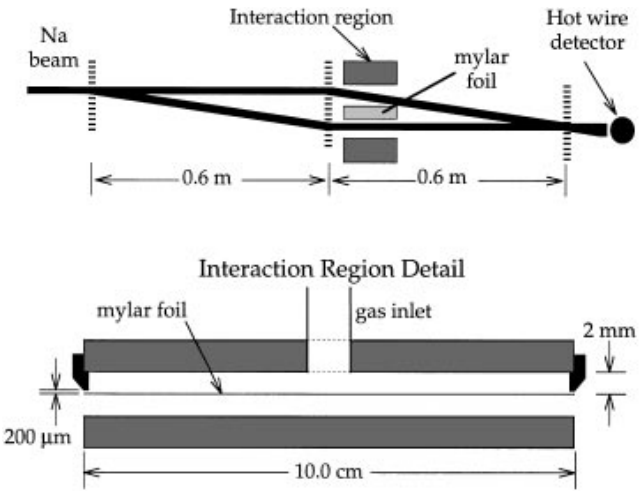

FIG. 1. Schematic of our interferometer and interaction region. Vertical dashed lines are 200 nm period diffraction gratings. The detail of the interaction region shows the 10 μm mylar foil suspended between the side plates. The side plates that form the gas cell are indicated in black at both ends.

diffraction grating, centered on the zeroth order peak. Thus, one of the two symmetric first diffracted orders passed through the gas, while the other first order passed through the empty side of the interaction region. Gas was then leaked into the interaction region and the attenuation of both beams was measured as a function of pressure rise in the main vacuum chamber as recorded on an ionization gauge. This gauge reading is not meant to be an accurate measure of the column density, only a reproducible linear measure of relative column density. The attenuation as a function of gauge reading for both beams was fit to an exponential. Comparing the measured attenuation for Ar, Kr, and Xe to the cross sections calculated from the potentials in Ref. [12] allows us to estimate the density of the gas in our interaction region.

In the second experiment the amplitude A of the interference pattern and the phase shift $\Delta\phi$ were measured with various gas densities in one arm of the atom interferometer. This was achieved by repositioning the mylar foil between the two beams of the atom interferometer. In this configuration, the stronger zeroth order beam passes through the gas sample and has its amplitude attenuated and its phase shifted. Interference patterns were first recorded for zero gas flow, then for a particular pressure rise in the main chamber, and then zero again. The phase shift and interference amplitude were determined and recorded for each value of the pressure rise, with the mean of the zero values providing the baseline. The measured phase shift was found to be a linear function of the pressure rise (Fig. 2).

Because we do not have a good absolute measure of the column density N_c, we were most accurately able to determine the ratio of the real and imaginary parts of the

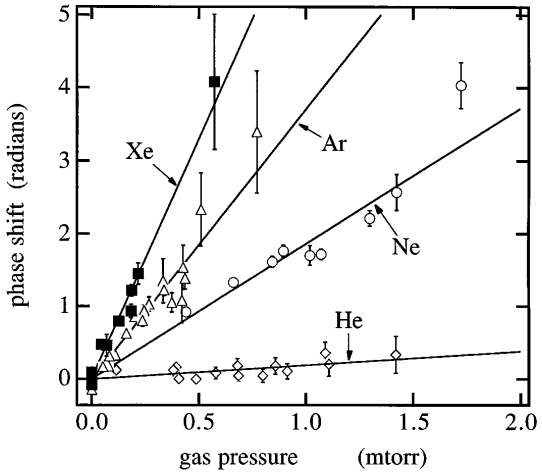

FIG. 2. Phase shift of Na matter waves passing through He, Ne, Ar, and Xe gas as a function of the estimated gas pressure in the cell.

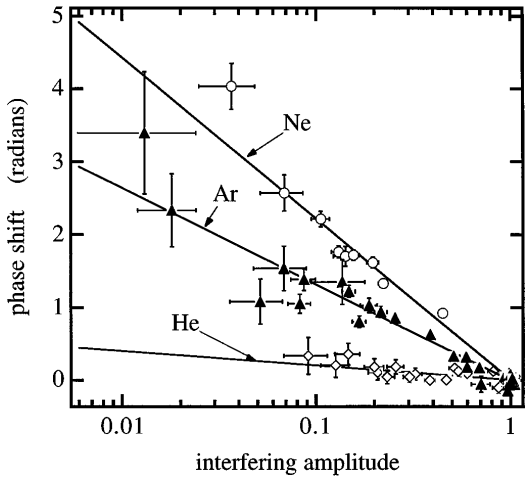

FIG. 3. Phase shift of Na matter waves plotted vs the interfering amplitude when passing through He, Ne, and Ar in the gas cell. The slope of the fitted line is a direct measurement of the ratio $\mathrm{Re}[f(k,0)]/\mathrm{Im}[f(k,0)]$.

forward scattering amplitude from simultaneous measurements of the attenuation of the interfering amplitude A and the phase shift $\Delta\varphi$ in the interferometer:

$$\frac{-\Delta\varphi(N_c)}{\ln[A(N_c)/A(0)]} = \frac{\mathrm{Re}[f(k,0)]}{\mathrm{Im}[f(k,0)]}. \tag{3}$$

The ratio of the real and imaginary parts of the forward scattering amplitude is then the slope of the phase shift plotted as a function of the natural logarithm of the interfering amplitude (Fig. 3). Since both A and $\Delta\varphi$ can simultaneously be determined from the same interference scan, this method does not rely on a pressure measurement at all. This procedure also takes advantage of the fact that the interference amplitude decreases only as the square root of the intensity in the attenuated beam [13] and is therefore easier to measure at high pressures (where the intensity is attenuated by up to a factor of 1000).

We measured this ratio for the various monatomic rare gases He, Ne, Ar, Kr, and Xe and for the molecular gases N_2, CO_2, NH_3, and H_2O (Table I). It is noteworthy that the measured (phase shifts)/torr vary by a factor of 13, whereas the total scattering cross sections vary only by a factor of 4.

Since this is the first time that $\mathrm{Re}[f(k,0)]$ has been measured for atom-atom scattering, it is important to consider some simple models illustrating its behavior.

The simplest case is a hard sphere with radius r_H. The partial wave phase shifts are given by $\tan(\delta_l) = j_l(kr_H)/n_l(kr_H)$ [14], and the sum over angular momentum can be evaluated numerically. Partial waves whose classical impact parameter $b = (l + \frac{1}{2})/k$ just exceeds r_H are systematically repelled. Therefore the ratio of real to imaginary parts of the scattering amplitude is always negative. Numerical calculations show that it roughly equals the inverse of the square root of the number of partial waves contributing to the scattering process: $\mathrm{Re}[f(k,0)]/\mathrm{Im}[f(k,0)] \approx -1/\sqrt{kr_H}$.

Next we consider a long range attractive interaction potential of the form $C_n r^{-n}$. Calculating the partial wave

TABLE I. Phase shift $\Delta\varphi$, refractive index n, and the ratio $\mathrm{Re}[f(k,0)]/\mathrm{Im}[f(k,0)]$, for 1000 m/s Na atoms passing through various gases at 300 K and 1 mtorr pressure. The data are compared to JWKB calculations using 6-8 [15] and 6-12 [12] potentials.

	Experiment			Calculations $\mathrm{Re}(f)/\mathrm{Im}(f)$	
Gas	$\Delta\varphi(\mathrm{mtorr}^{-1})$	$10^{10}(n-1)\,(\mathrm{mtorr}^{-1})$	$\frac{\mathrm{Re}(f)}{\mathrm{Im}(f)}$	6-8 pot.	6-12 pot.
He	0.50	$0.14 + 1.18i$	0.12(2)		
Ne	2.0	$0.55 + 0.56i$	0.98(2)	1.24	
Ar	3.9	$1.07 + 1.81i$	0.59(3)		0.69
Kr	5.4	$1.51 + 2.45i$	0.62(6)	0.75	0.73
Xe	6.5	$1.81 + 2.49i$	0.73(3)	0.76	0.73
N_2	4.7	$0.91 + 1.39i$	0.60(2)		
NH_3	3.3	$1.30 + 2.16i$	0.65(4)		
CO_2	5.0	$1.37 + 2.21i$	0.62(2)		
H_2O	6.2	$1.71 + 2.40i$	0.72(3)		

phase shifts in eikonal approximation, and converting the partial wave sums in Eq. (2) into integrals over impact parameter, we find for any r^{-n} attractive potential:

$$\frac{\mathrm{Re}[f(k,0)]}{\mathrm{Im}[f(k,0)]} = -(n-1) \times \frac{\Gamma\left(\frac{1}{2} - 1/(n-1)\right)\Gamma\left(\frac{1}{2} + 1/(n-1)\right)}{\Gamma\left(-1/(n-1)\right)\Gamma\left(1/(n-1)\right)}. \quad (4)$$

This ratio is independent of the strength of the potential and center of mass energy, which follows because no length scale is defined in this problem. It depends strongly on n (Table II). For neutral atoms in s states one would expect the long range tail of the actual potential to be a van der Waals interaction, $V_{\mathrm{vdW}}(r) = -C_6 r^{-6}$ in which case we would expect $\mathrm{Re}[f(k,0)]/\mathrm{Im}[f(k,0)] \cong 0.72$.

We can say several qualitative things about the scattering we have observed. First of all, the depth of the minimum of the interatomic potential varies considerably from He to Xe. Helium has the weakest long range attraction, a very shallow minimum, and behaves most like a hard sphere. The ratio $\mathrm{Re}[f(k,0)]/\mathrm{Im}[f(k,0)]$ is very small, but its positive sign gives clear evidence of an attractive long range interaction. The Na-Xe potential, on the other hand, has a well deep enough to generate many radians of phase, and so the long range part of the potential should dominate. Its ratio comes closest to the value expected for a long range r^{-6} interaction. The values measured for the other gases deviate progressively further from this ratio as the well depth decreases (which it does monotonically with decreasing mass of the rare gas).

To make a more detailed comparison of our results with theory we used the JWKB approximation to calculate the forward scattering amplitude from modified 6-12 potentials [12] and 6-8 potentials [15] determined from scattering and spectroscopic data. The calculations show that the large ratio of real to imaginary part for Na-Ne results from the fact that the maximum of the phase shift near the potential minimum is never larger than one radian, generating a large contribution to the sum for Eq. (2a). For the much stronger Na-Kr and Na-Xe interactions the calculations give nearly the same results as the van der Waals potential (Table I). Nevertheless, significant discrepancies remain, especially for Na-Ne and Na-Ar, between our experiments and the predictions based on potentials obtained by standard scattering experiments [3,12,15] indicating the need to refine these potentials. Considerably more effort is required to understand the molecular data.

As we have shown, measurement of collisional phase shifts provides a fundamentally different probe of scattering processes than measurement of total cross sections that is especially sensitive to the long range shape of the interatomic potential. In the future we hope to improve the sensitivity of this method by studying the velocity dependence of the forward scattering amplitude $f(k,0)$, to extract more detailed information about the scattering potentials. We also hope to study the effects of inelastic processes and excitations in forward scattering. These should cause a reduction in the ratio of $\mathrm{Re}[f(k,0)]/\mathrm{Im}[f(k,0)]$ if they occur at large impact parameters (but no evidence for this is seen here). Other possibilities include modifications of the forward scattering amplitude by external fields, and a direct measurement of the sign of the atom-atom scattering lengths using cold atoms.

TABLE II. The ratio $\mathrm{Re}[f(k,0)]/\mathrm{Im}[f(k,0)]$ as calculated for a long range $1/r^n$ potential.

n	5	6	7	8
$\mathrm{Re}[f(k,0)]/\mathrm{Im}[f(k,0)]$	1.00	0.72	0.58	0.48

This work was supported by the Army Research Office Contracts No. DAAL03-89-K-0082 and No. ASSERT 29970-PH-AAS, the Office of Naval Research Contract No. N00014-89-J-1207, and the Joint Services Electronics Program Contract No. DAAL03-89-C-0001. J. S. was partly supported by an APART fellowship of the Austrian Academy of Sciences, and T. H. acknowledges the support of a National Science Foundation Graduate Research Fellowship. We thank B. Tannian for technical assistance. We also thank Michael Rooks and other staff at the National Nanofabrication Facility at Cornell University for their help in grating fabrication.

[1] For an overview, see D. E. Pritchard, in *ICAP XIII* (1992); Special issues on *Optics and Interferometry with Atoms*, edited by J. Mlynek, V. Balykin, and P. Meystre [Appl. Phys. B **54**, (1992)]; edited by J. Boudon and Ch. Mineatura [J. Phys. II, (1994)].

[2] J. Schmiedmayer *et al.*, in *Fundamentals of Quantum Optics III*, edited by F. Ehlotzky, Springer Lecture Notes in Physics 420 (Springer-Verlag, Berlin, 1993).

[3] R. Düren, Adv. At. Mol. Phys. **16**, 55 (1980).

[4] K. Chadan and P. C. Sabatier, *Inverse Problems in Quantum Scattering Theory* (Springer, New York, 1989).

[5] R. A. Cline, J. M. Miller, and D. J. Heinzen, Phys. Rev. Lett. **73**, 632 (1994); P. D. Lett *et al.*, Phys. Rev. Lett. **71**, 2200 (1993); V. Bagnato *et al.*, Phys. Rev. Lett. **70**, 3225 (1993); T. Walker and P. Feng, Adv. At. Mol. Opt. Phys. (to be published).

[6] H. T. C. Stoof, Phys. Rev. Lett. **66**, 3148 (1991); A. J. Moerdijk, W. C. Stwalley, R. G. Hulet, and B. J. Verhaar, Phys. Rev. Lett. **72**, 40 (1994); A. J. Moerdijk and B. J. Verhaar, Phys. Rev. Lett. **73**, 518 (1994).

[7] H. Lichte, Physica (Amsterdam) **151B**, 214 (1988).

[8] V. F. Sears, *Neutron Optics* (Oxford University Press, Oxford, 1990).

[9] For an overview of Neutron Interferometry, see G. Badurek, H. Rauch, and A. Zeilinger, Physica **151B**,

82 (1988); experiments measuring the refractive index of gases are described in H. Kaiser *et al.*, Z. Phys. A **291**, 231 (1979).

[10] D. W. Keith, C. R. Ekstrom, Q. A. Turchette, and D E. Pritchard, Phys. Rev. Lett. **66**, 2693 (1991).

[11] C. R. Ekstrom, D. W. Keith, and D. E. Pritchard, App. Phys. B **54**, 369 (1992).

[12] U. Buck and H. Pauly, Z. Phys. **208**, 390 (1968); R. Düren, G. P. Raabe, and C. Schlier, Z. Phys. **214**, 410 (1968).

[13] H. Rauch, J. Summhammer, M. Zawisky, and E. Jericha, Phys. Rev. A **42**, 3726 (1990).

[14] J. J. Sakurai, *Modern Quantum Mechanics* (Addison-Wesley, Reading, MA, 1985).

[15] P. Barwig, U. Buck, E. Hundhausen, and H. Pauly, Z. Phys. **196**, 343 (1966); R. Düren, A. Frick, and C. Schlier, J. Phys. B **5**, 1744 (1972); R. A. Gottscho *et al.*, J. Chem. Phys. **75**, 2546 (1981).